Journal of the Korean Nuclear Society
Volume 35, Number 3, pp.214~225, June, 2003

Development of a Teleoperated Manipulator System for Remote Handling of Spent Fuel Bundles

Sung Ho Ahn, Jae Hyun Jin, and Ji Sup Yoon
Korea Atomic Energy Research Institute
150 Dukjin-dong, Yuseung-gu, Daejeon 305-353, Korea
shahn2@kaeri.re.kr

(Received November 13, 2002)

Abstract

A teleoperated manipulator system has been developed for remote handling of the spent fuel bundles. A heavy-duty power manipulator with high reduction ratio joints is used for the slave manipulator in the developed system since the handling tasks of the spent fuel bundles need power. Also, the universal type master manipulator, which has force reflecting capability, is used for precise remote manipulation. The power manipulators so frequently occur the control input saturation that the precise control performances are not achieved due to the windup phenomenon. An advanced bilateral control scheme compensating for the saturation is applied to the teleoperated manipulator system. The validity of the developed system is verified by the grid cutting and fuel transportation tasks from the mockup spent fuel bundle.

Key Words : teleoperation, remote handling, spent fuels, manipulator, bilateral control

1. Introduction

The handling and dismantling tasks of spent fuel bundles are usually performed with the teleoperated manipulator systems since the tasks are carried out in high radiation areas. The teleoperated manipulator system is the master-slave manipulator system, in which the operator controls the slave manipulator located in a remote area by means of manipulating the master manipulator. The teleoperated system presents a technical alternative for intelligent robotic systems performing dexterous tasks in unstructured environments such as in a nuclear facility, outer space and underwater. Since teleoperated systems include continuous human intervention into the control loop, it is important to provide realistic sensory feedback of the environmental interactive forces to the operator.

The electromechanical type force reflecting servo manipulators have been developed, applying to the nuclear industry since the first teleoperated manipulator system was introduced by ANL of U.S.A in 1945, which was the mechanical type master-slave system and used for handling of radioactive materials [1,2]. However, these manipulators have a low weight-to-payload ratio (payload: $10\sim25kgf$), which make them

unsuitable for many potential application areas of the nuclear industry even though these have the force reflecting capability to improve the efficiency of remote manipulation.

To achieve a sensitive force reflection capability, it is generally required for the slave manipulator to have a drive mechanism with low reduction gears. On the other hand, manipulators consisting of high reduction ratio joints are widely applied in heavy-duty tasks even though it reveals nonlinear properties such as actuator saturation, nonlinear stiffness and friction, etc. [3]. For example, Hans Wälischmiller A1065 of Germany and GCA 300 of U.S.A [4] have been widely used for remote handling and transportation of high radioactive materials even though these are not applied to the tasks needed for precision since these consist of high reduction ratio joints and are unilaterally operated. The handling and dismantling of spent fuel bundles are in such an area that it critically requires the use of slave manipulators with a high payload because the tasks undergo intensive interactive forces.

When a manipulator consisting of high reduction ratio joints is used as the slave manipulator in teleoperated systems, the control input is frequently saturated because the dynamics of the slave manipulator with high reduction ratio joints is likely to be much slower than that of the master manipulator. If the control input of the slave manipulator is saturated in the teleoperated systems, the system stability and position tracking performance of the slave manipulator are deteriorated due to the windup phenomenon caused by the saturation [5,6]. Thus, the precise control performance of the slave manipulator cannot be achieved because its end-effector can be moved regardless of the operator's intention.

KAERI (Korea Atomic Energy Research Institute) has developed a teleoperated manipulator system for the study of the remote handling of a spent fuel mockup bundle. In this paper, the developed manipulator system and its performance test results are presented. The developed manipulator system has an enhanced bilateral control scheme, which improves the position tracking and force reflecting performances while compensating for the windup phenomenon. The developed manipulator system is applied to the remote cutting tasks of mockup spent fuel bundle. The developed manipulator system is introduced in section 2, and an enhanced bilateral control scheme is presented in section 3. The experimental results are presented in section 4.

2. Developed Manipulator System

2.1. System Composition

Fig. 1 shows the block diagram of the developed manipulator system for remote handling of spent fuel bundles. The system consists of a master manipulator, slave manipulator, F/T (Force/Torque) sensor, control system, etc. In the developed system, the end-effector of the slave manipulator located in the remote area is controlled by an operator through the master manipulator, while the contact forces/torques sensed by the F/T sensor at the end-effector of the slave manipulator are reflected back to the

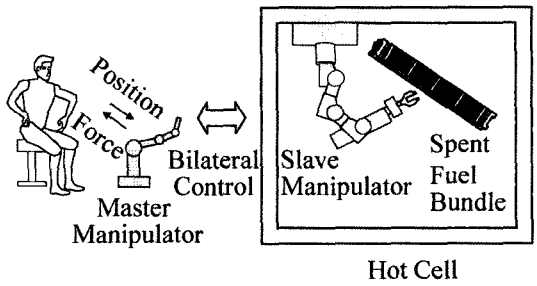

Fig. 1. Block Diagram of the Teleoperated Manipulator System

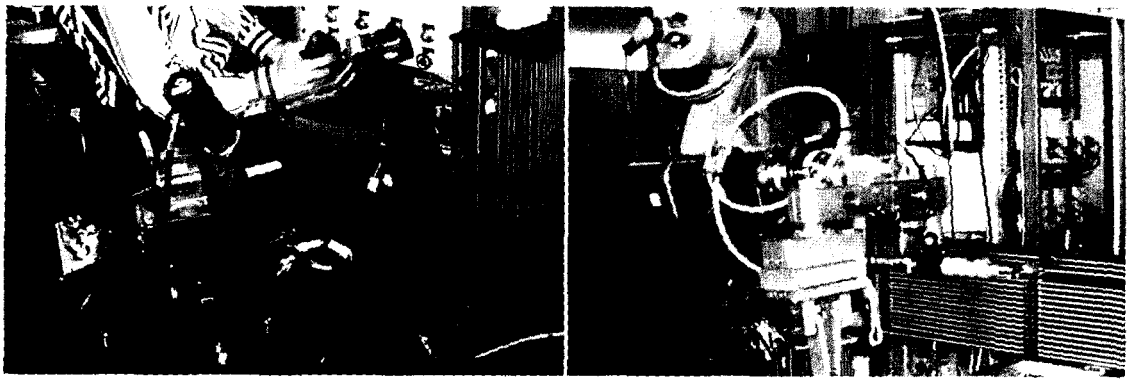

(a) Master manipulator (b) Slave manipulator

Fig. 2. Picture of the Developed Manipulator System

operator through the master manipulator. Fig. 2 shows the picture of the developed system. The master manipulator is the universal type 6-DOF manipulator with force reflecting capability. It consists of a serial and string & pulley type driving structure and is installed on the right armrest part of the chair.

The operator can manipulate the master manipulator in up and down directions, left and right turns, and forward and backward direction sitting in the chair. The slave manipulator is a heavy-duty power manipulator, which is manufactured by the Hans Wälischmiller and has 7-DOF with high reduction ratio reducers and a payload of 100*kgf*. It is attached to the telescopic mast installed in the trolley, which is movable in X and Y directions. It is used for heavy-duty tasks such as remote handling and transporting of radwaste materials. The handling tool is attached in the end-effector of the slave manipulator, which is equipped with an air operated shears and a gripper. The F/T sensor is installed at the end-effector of the slave manipulator to measure the contact force between the slave manipulator and the environment. The specifications of the F/T sensor are summarized in Table 1.

The control system consists of a PC equipped with a multi-axis motion controller, and interconnected with the motor drivers of each master and slave manipulators. The control system obtains the angular positions from the encoder installed at each axis of the master and slave

Table 1. Specifications of F/T Sensor

Model No.	F/T 160/2400, BL Autotec. Inc.	
Capacity	Force (kgf)	160
	Torque (kgf-cm)	2400
Resolution	Fx, Fy (kgf)	0.125
	Fz (kgf)	0.375
	Tx, Ty, Tz (kgf-cm)	1.2

Table 2. Specifications of Motors

	Joint	Capacity (W)	Max. Torque (N-m)	Rated Speed (rpm)	Reduction Ratio
Slave	1	420	1.25	4000	1:120
	2	420	1.25	4000	1:80
	3	270	0.85	4000	1:80
Master	1	800	7.6	3000	1:1
	2	800	7.6	3000	1:3
	3	200	1.9	3000	1:1

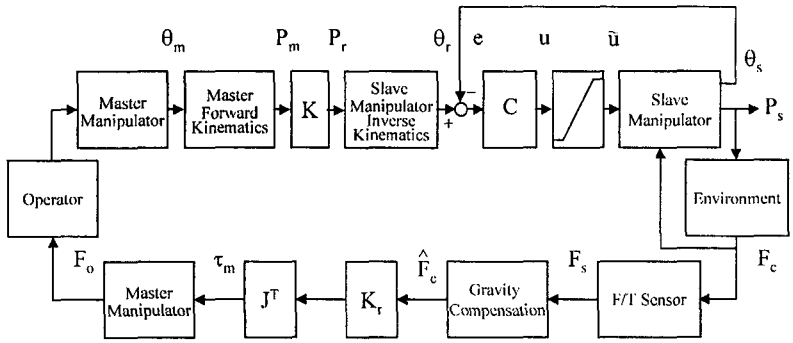

Fig. 3. Conventional Bilateral Control Scheme with Control Input Saturation

manipulator, and obtains the contact forces from the F/T sensor. Also, the control system controls the position of the end-effector of the slave manipulator to track the reference position designated by the master manipulator, and provides force reflection of the contact forces to the operator. The 3-DOF of the master manipulator and that of the slave manipulator are interconnected for remote handling of the mockup spent fuel bundle. The specifications of the motors used in the master and slave manipulators are summarized in Table 2.

2.2. System Characteristics

The conventional bilateral control scheme for a heavy-duty power manipulator with high reduction ratio joints is shown in Fig. 3 [7]. Since the dynamics of the velocity controlled 3-DOF slave manipulator with high reduction ratio joints is very slow, the coupling effect in controlling of the joint angular position can be ignored. In Fig. 3, $C(s)$ is given by

$$C(s) = diag\left[C_1(s), C_2(s), C_3(s)\right]. \quad (1)$$

Where $C_i(s), i=1,2,3$ are the controllers for each axis of the slave manipulator.

When a heavy-duty power manipulator with high reduction ratio joints is used as the slave manipulator in the teleoperated system, the actuators of the slave manipulator are frequently saturated. $\tilde{u}_i(t)$ have the following saturation characteristic

$$\tilde{u}_i(t) = \begin{cases} u_{i\max} & u_i(t) > u_{i\max} \\ u_i(t) & -u_{i\max} \le u_i(t) \le u_{i\max} \\ -u_{i\max} & u_i(t) < -u_{i\max} \end{cases}, i = 1,2,3. \quad (2)$$

The system stability and position tracking performance of the slave manipulator are deteriorated by the windup phenomenon caused by saturation. Especially, when the multi-DOF master and slave manipulators are interconnected, the movements of each link of the master and slave manipulators are not always coincidental because the positions of each manipulator are related to kinematics or inverse kinematics. Consequently, it is very difficult to obtain the positional coincidence between the handgrip of the master manipulator and the end-effector of the slave manipulator when the actuators of the slave manipulator are saturated. Moreover, the end-effector of the slave manipulator can contact with an object regardless of the operator's intention and a precise control performance with force reflection cannot be obtained.

3. Controller Design

3.1. Kinematics Analysis and Workspace Mapping

Fig. 4 shows the schematic diagrams of each 3-DOF master and slave manipulator for the developed system. For the workspace mapping, l_{m1} and l_{s1} are set at zero respectively, and K is set at 1. In other words, the end-effector position of the slave manipulator tracks the handgrip position of the master manipulator while the link length of each axis 1 of master and slave manipulator is ignored.

The position transformation matrix of the master manipulator is solved by D-H (Denavit-Hatenberg) notation [8] in Fig. 4, (a), and given by

$$ {}^{0}_{3}T = \begin{bmatrix} r_{11} & r_{12} & r_{13} & x_m \\ r_{21} & r_{22} & r_{23} & y_m \\ r_{31} & r_{32} & r_{33} & z_m \\ 0 & 0 & 0 & 1 \end{bmatrix}. \quad (3) $$

For Eg. (3), the rotation matrix, r_{ij}, $(i,j = 1,2,3)$ is given by

$$ r_{ij} = \begin{bmatrix} C_{m1}C_{m23} & -C_{m1}S_{m23} & S_{m1} \\ S_{m1}C_{m23} & -S_{m1}S_{m23} & -C_{m1} \\ S_{m23} & C_{m23} & 0 \end{bmatrix}, \quad (4) $$

and the position vector of handgrip with l_{m1} is solved by the forward kinematics of master manipulator and given by

$$ \begin{bmatrix} x_m \\ y_m \\ z_m \end{bmatrix} = \begin{bmatrix} C_{m1}(C_{m2}l_{m2} + C_{m23}l_{m3}) \\ S_{m1}(C_{m2}l_{m2} + C_{m23}l_{m3}) \\ S_{m2}l_{m2} + S_{m23}l_{m3} \end{bmatrix}. \quad (5) $$

Where $C_{mi} = \cos\theta_{mi}$, $S_{mi} = \sin\theta_{mi}$, $C_{mij} = \cos(\theta_{mi}+\theta_{mj})$, $S_{mij} = \sin(\theta_{mi}+\theta_{mj})$.

The reference angular position, which is to be moved by each axis of the slave manipulator, is given by solving the inverse kinematics of the slave manipulator. The position transformation matrix of the slave manipulator is solved by D-H notation in Fig. 4, (b), and given by

$$ {}^{0}_{3}T = \begin{bmatrix} r_{11} & r_{12} & r_{13} & x_s \\ r_{21} & r_{22} & r_{23} & y_s \\ r_{31} & r_{32} & r_{33} & z_s \\ 0 & 0 & 0 & 1 \end{bmatrix}. \quad (6) $$

For Eq. (6), the rotation matrix, r_{ij},$(i,\ j=1,2,3)$, is given by

$$ r_{ij} = \begin{bmatrix} C_{s1}C_{s23} & -C_{s1}S_{s23} & S_{s1} \\ S_{s1}C_{s23} & -S_{s1}S_{s23} & -C_{s1} \\ S_{s23} & C_{s23} & 0 \end{bmatrix}, \quad (7) $$

and the position vector of end-effector for the

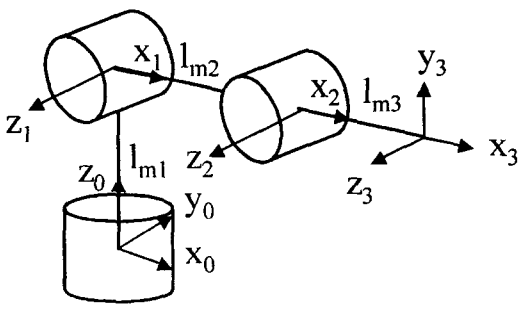

(a) Master manipulator

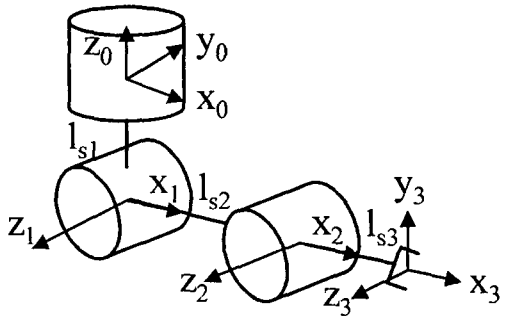

(b) Slave manipulator

Fig. 4. Schematic Diagrams of the 3-DOF Master and Slave Manipulators

position vector of axis 1 with $l_{s1} = 0$ is given by

$$\begin{bmatrix} x_s \\ y_s \\ z_s \end{bmatrix} = \begin{bmatrix} C_{s1}(C_{s2}l_{s2} + C_{s23}l_{s3}) \\ S_{s1}(C_{s2}l_{s2} + C_{s23}l_{s3}) \\ S_{s2}l_{s2} + S_{s23}l_{s3} \end{bmatrix}. \quad (8)$$

Where $C_{si} = \cos\theta_{si}$, $S_{si} = \sin\theta_{si}$, $C_{sij} = \sin(\theta_{si}+\theta_{sj})$. The reference angular position, which is moved by each axis of the slave manipulator, is given by Eq. (9) by solving the inverse kinematics of the slave manipulator from $[x_s\ y_s\ z_s]^T$.

$$\begin{bmatrix} \theta_{r1} \\ \theta_{r2} \\ \theta_{r3} \end{bmatrix} = \begin{bmatrix} A\tan 2(y_s, x_s) \\ A\tan 2(\mp\sqrt{1-C_{s2}^2}, C_{s2}) \\ A\tan 2(\pm\sqrt{1-C_{s3}^2}, C_{s3}) \end{bmatrix}. \quad (9)$$

Where

$$C_{s2} = \frac{(C_{s1}x_s + S_{s1}y_s)(l_{s2} + C_{s3}l_{s3}) + S_{s3}l_{s3}z_s}{(l_{s2} + C_{s3}l_{s3})^2 + (S_{s3}l_{s3})^2}, \quad (10)$$

$$C_{s3} = \frac{(C_{s1}x_s + S_{s1}y_s)^2 + z_s^2 - l_{s2}^2 - l_{s3}^2}{2l_{s2}l_{s3}}. \quad (11)$$

The torques generated at each axis of the master manipulator for reflecting the contact force to the operator is achieved by solving J^T, and J^T is given by [9]

$$J^T = \begin{bmatrix} 0 & S_{m3}l_{m2} & 0 \\ 0 & C_{m3}l_{m2} + l_{m3} & l_{m3} \\ -C_{m2}l_{m2} - C_{m23}l_{m3} & 0 & 0 \end{bmatrix}. \quad (12)$$

3.2. Advanced Bilateral Control Scheme

In this section, an enhanced bilateral control scheme is proposed for the developed manipulator system, which provides effective position tracking and force reflection performances regardless of actuator saturation. The enhanced scheme is shown in Fig. 5. The main features of the enhanced scheme are as follows: (1) the controllers for each axis of the slave manipulator are designed with an anti-windup scheme, and (2) the nonlinear properties of the actuator saturation are then treated as another contact and the equivalent forces are also reflected to the operator to prevent fast manipulation of the master handgrip.

The controllers for each axis of the slave manipulator are designed with the following two-step design procedure [5].

First step: $C_i(s)$ in Eq. (1) are designed by the following PID controller.

$$C_i(s) = K_{Pi} + \frac{K_{Ii}}{s} + \frac{K_{Di}s}{s+\gamma_i}, i = 1,2,3, \quad (13)$$

where $C_i(s)$ are designed to be a biproper and minimum phase, and the PID parameters of $C_i(s)$ are set to guarantee the position tracking performance without considering the saturation.

Second step: $C_a(s)$ and $C_b(s)$ in Fig. 5 are designed as follows.

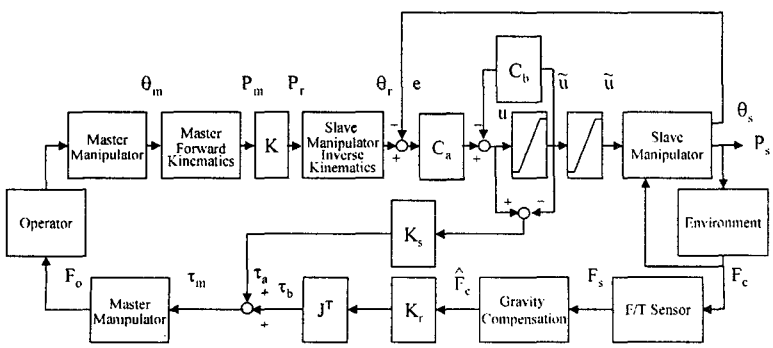

Fig. 5. An Enhanced Bilateral Control Scheme Compensating the Saturatuion

$$C_a(s) = diag[C_{a1}(s), C_{a2}(s), C_{a3}(s)], \quad (14)$$

where $C_{ai}(s)$, $i = 1,2,3$ are designed to be a biproper, minimum phase and stable, and

$$C_b(s) = diag[C_{b1}(s), C_{b2}(s), C_{b3}(s)], \quad (15)$$

$$C_{bi}(s) = C_{ai}(s)C_i^{-1}(s) - 1, \ i = 1,2,3. \quad (16)$$

Then, the controller composed of $C_a(s)$ and $C_b(s)$ acts as the anti-windup controller in the saturated condition as well as acting as $C(s)$ without cancellaton of unstable poles and zeros in the non-saturated condition [5].

In order to improve the position tracking performance, the proposed bilateral control scheme has a force reflection loop caused by the actuator saturations in addition to the general force reflection loop. If the actuators are saturated under the non-contact condition in Fig. 5, the following torques, which are caused by saturation, are generated in the joints of the master manipulator

$$\begin{bmatrix} \tau_{m1}(s) \\ \tau_{m2}(s) \\ \tau_{m3}(s) \end{bmatrix} = \begin{bmatrix} \tau_{a1}(s) \\ \tau_{a2}(s) \\ \tau_{a3}(s) \end{bmatrix} = K_s \begin{bmatrix} |u_1(s) - \tilde{u}_1(s)| \\ |u_2(s) - \tilde{u}_2(s)| \\ |u_3(s) - \tilde{u}_3(s)| \end{bmatrix}. \quad (17)$$

Where

$$K_s = \begin{bmatrix} a_1 K_{s11} & a_1 K_{s12} & a_1 K_{s13} \\ a_2 K_{s21} & a_2 K_{s22} & a_2 K_{s23} \\ a_3 K_{s31} & a_3 K_{s32} & a_3 K_{s33} \end{bmatrix}, \quad (18)$$

$$a_i = \begin{cases} +1, \text{if } \theta_{mi} \text{ is increasing} \\ -1, \text{if } \theta_{mi} \text{ is decreasing} \\ 0, \text{if } \theta_{mi} \text{ is not changing} \end{cases}, \ i = 1,2,3. \quad (19)$$

The actuator saturations of the slave manipulator are caused by the fast movement of links of the master manipulator in the bilateral control system. The joint torques given by Eq. (17) generate the reflected forces to the operator through the links of the master manipulator, which are moving, whenever any actuator for an axis of the slave manipulator is saturated. Thus, the operator can manipulate slow or suspended motion of the handgrip of the master manipulator for the saturation. When the position change of the handgrip is a limited value, the steady state tracking error of the slave manipulator for the reference position is zero for both the non-contact and contact cases [5]. Consequently, the end-effector of the slave manipulator has a good position tracking performance for the reference position, while the windup phenomenon is compensated for.

If the end-effector of the slave manipulator contacts an object under the non-saturated condition, the following torques are generated in the master manipulator caused by the contact

$$\begin{bmatrix} \tau_{m1}(s) \\ \tau_{m2}(s) \\ \tau_{m3}(s) \end{bmatrix} = \begin{bmatrix} \tau_{b1}(s) \\ \tau_{b2}(s) \\ \tau_{b3}(s) \end{bmatrix} = J^T K_r \begin{bmatrix} \hat{F}_{cx}(s) \\ \hat{F}_{cy}(s) \\ \hat{F}_{cz}(s) \end{bmatrix}. \quad (20)$$

Where J^T is given by Eq. (12). Thus, the contact forces are reflected to the operator through the joint torques as conventional bilateral control schemes.

If the end-effector of the slave manipulator contacts an object under the saturated condition, the following torques caused by saturation as well as contact are generated in the master manipulator while compensating for the windup phenomenon.

$$\begin{bmatrix}\tau_{m1}(s)\\ \tau_{m2}(s)\\ \tau_{m3}(s)\end{bmatrix}=\begin{bmatrix}\tau_{a1}(s)\\ \tau_{a2}(s)\\ \tau_{a3}(s)\end{bmatrix}+\begin{bmatrix}\tau_{b1}(s)\\ \tau_{b2}(s)\\ \tau_{b3}(s)\end{bmatrix}. \quad (21)$$

Since the controllers for axes of the slave manipulator are designed with an anti-windup feature, the actuators of the slave manipulator are not saturated in the steady state under the contact condition for the operator's bounded position command. Therefore, when the operator retracts the handgrip of the master manipulator under the contact condition, the end-effector of the slave manipulator rapidly tracks to the reference position. Consequently, the end-effector position of the slave manipulator can be precisely controlled regardless of contact and saturation.

3.3. Gravity Compensation

The F/T sensor installed at the end-effector of the slave manipulator generates values even though the slave manipulator is not contacted. Moreover, the F/T sensor signal is changed depending on the position due to the influence of the gravity. Thus the effect of the gravity in the F/T sensor signal should be compensated. The contact force which is derived by compensating the gravity from the F/T sensor signal, is given by

$$\hat{F}_c(s)=K_{co}\{F_s(s)-F_g(s)\}, \quad (22)$$

where K_{co} is the correction coefficient and

$$\hat{F}_c(s)=\left[\hat{F}_{cx}(s)\ \hat{F}_{cy}(s)\ \hat{F}_{cz}(s)\right]^T, \quad (23)$$

$$F_s(s)=\left[F_{sx}(s)\ F_{sy}(s)\ F_{sz}(s)\right]^T, \quad (24)$$

$$F_g(s)=\left[F_{gx}(s)\ F_{gy}(s)\ F_{gz}(s)\right]^T. \quad (25)$$

$F_g(s)$ is calculated from the initial end-effector position of the slave manipulator as follow [8]

$$\begin{bmatrix}F_{gx}(s)\\ F_{gy}(s)\\ F_{gz}(s)\end{bmatrix}=\begin{bmatrix}C_{s12} & -S_{s12} & 0\\ S_{s12} & C_{s12} & 0\\ 0 & 0 & 1\end{bmatrix}\begin{bmatrix}F_{ax}(s)\\ F_{ay}(s)\\ F_{az}(s)\end{bmatrix}. \quad (26)$$

Where $[F_{ax}(s)\ F_{ay}(s)\ F_{az}(s)]^T$ is the average value of the F/T sensor outputs at the initial position.

4. Experimental Results

The performance of the developed system is evaluated by a series of experiments. The actuator outputs of the slave manipulator have the following saturation characteristics for the calculated control inputs.

$$\tilde{u}_i(t)=\begin{cases}10V & u_i(t)>10V\\ u_i(t) & -10V\le u_i(t)\le 10V,\ i=1,2,\\ -10V & u_i(t)<-10V\end{cases} \quad (27)$$

$$\tilde{u}_3(t)=\begin{cases}5V & u_3(t)>5V\\ u_3(t) & -5V\le u_3(t)\le 5V.\\ -5V & u_3(t)<-5V\end{cases} \quad (28)$$

The developed teleoperated manipulator system is applied to the remote handling of a mockup spent fuel bundle. The dismantling tool, which consists of the air operated shears and the motor operated gripper, was installed in the end-effector of the slave manipulator for used for the grid plate cutting task and the fuel rod transportation task, respectively. K_r and K_s values were determined by a trial and error method considering the force reflecting capability and the operability of the spent fuel's remote handling tasks. It is shown in Fig. 6 (b) and 7 (b) that the gravity compensation method proposed in section 3.3 well removes the gravity effect from the F/T sensor signals.

Fig. 6 shows the experimental results for a conventional bilateral control scheme of Fig. 3 in the grid cutting task. In Fig. 6, the operator

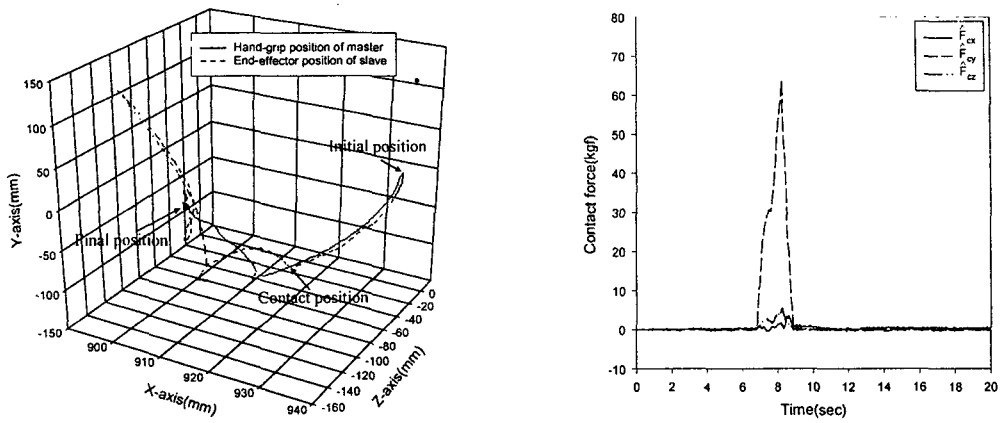

(a) Position tracking (b) Contact forces

Fig. 6. Responses for the Conventional Scheme in the Grid Cutting Task

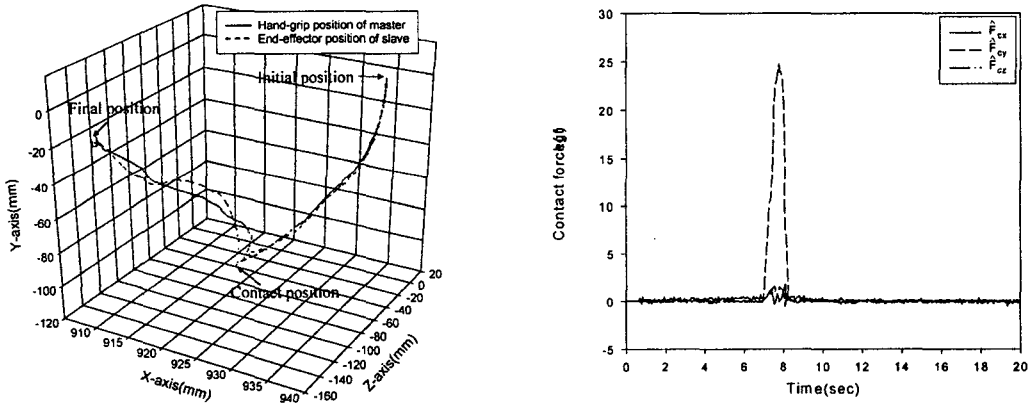

(a) Position tracking (b) Contact forces

Fig. 7. Responses for the Proposed Scheme in the Grid Cutting Task

manipulated the handgrip of the master manipulator that started from the initial position and moved to backward direction at the moment of sensing the reflected force caused by contact of slave manipulator, and then arrived at the final position. On the other hand, the end-effector of the slave manipulator started from the initial position and contacted to the grid plate, and arrived at the final position. It can be seen that the end-effector position of the slave manipulator tracks the handgrip position of the master manipulator with large error because the end-effector is unstably oscillated caused by the windup phenomenon of control input.

Fig. 7 shows the experimental results for the proposed scheme of Fig. 5 in the grid cutting task. In Fig. 7, the operator manipulated the handgrip of the master manipulator that started from the initial position moved to backward direction at the moment of sensing the reflected force caused by

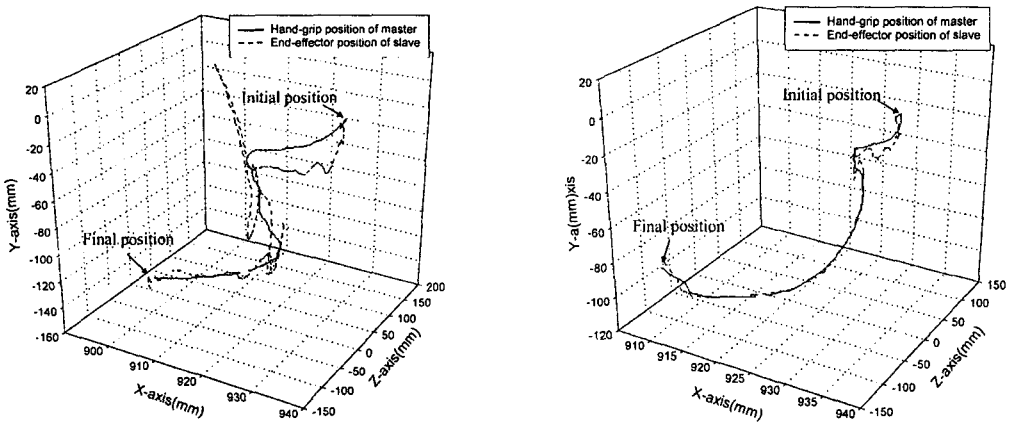

(a) Response for the conventional scheme

(b) Response for the proposed scheme

Fig. 8. Position Tracking Responses in the Fuel Transportation task

contact of slave manipulator, and then arrived at the final position. It is shown that the end-effector of the slave manipulator well tracks the handgrip position of the master manipulator regardless of the contact while compensating for the windup phenomenon.

Fig. 8 shows the experimental results for the responses in the fuel rod transportation task. Fig. 8 (a) shows the position tracking response for the conventional scheme without compensating the saturation. The operator manipulated the handgrip of the master manipulator that started from the initial position to the final position. On the other hand, the end-effector of the slave manipulator holding the fuel rod tracks the handgrip position with large error because the end-effector is unstably oscillated. Fig. 8 (b) shows the position tracking response for the proposed scheme by compensating for the saturation. It is shown in Fig. 8 (b) that the end-effector of the slave manipulator holding the fuel rod well tracks the handgrip position with small position error.

As a result, it is shown in Fig. 6 and Fig. 8 (a) that the conventional bilateral control scheme of Fig. 3 cannot be applied to the manipulator system for remote handling of the spent fuel bundle because it does not provide precise control performance. And it is concluded from Fig. 7 and Fig. 8 (b) that the manipulator system with the proposed bilateral control scheme provides precise position control and force reflecting performances in the remote handling tasks of the spent fuel bundle.

5. Conclusions

A teleoperated manipulator system, which was developed for remote handling of spent fuel bundle was presented in this paper. The heavy-duty power manipulator used for a slave manipulator frequently causes saturation in the control input that the precise control performance is not achieved due to the windup phenomenon even though it has a high payload. An advanced bilateral control scheme compensating for the saturation was applied for the teleoperated manipulator system. The developed universal type master manipulator enables the operator to manipulate the slave manipulator precisely while providing the force reflecting capability. The

performance of the developed system was verified by a series of experiments. The developed manipulator system has an advantage that the slave manipulators with high reduction ratio joints can be precisely controlled with force reflection and the safety is improved in remote tasks of hotcell facilities. In further studies, a force reflecting and compliance control scheme compensating for the saturation will be developed for the teleoperated manipulator system.

Acknowledgement

This research has been carried out as a part of the nuclear R&D program funded by the Ministry of Science and Technology in Korea.

Nomenclature

- C controller of the slave manipulator
- e angular position error
- F_c contact force between the slave manipulator and the environment
- $\hat{F}_c$ calculated contact force compensating the gravity
- F_o reflection force to the operator
- F_s force from the F/T sensor
- J^T jacobian transpose matrix for the master manipulator
- K position command scale factor
- K_r force reflection scale factor for the contact force
- K_s force reflection scale factor considering the actuator saturation
- l_{mi} i-th link length of the master manipulator
- l_{si} i-th link length of the slave manipulator
- P_m handgrip position of the master manipulator
- P_r reference position
- P_s end-effector position of the slave manipulator
- u calculated control input from the controller
- $\tilde{u}$ actual control input of the slave manipulator
- θ_m joint angular position of the master manipulator
- θ_r reference angular position
- θ_s joint angular position of the slave manipulator
- τ_m joint torque of the master manipulator
- τ_a joint torque of the master manipulator caused by saturation
- τ_b joint torque of the master manipulator caused by the contact force

References

1. S. Kawatsuma, et al., "The status of two-arm bilateral servomanipulator system development," *Proc. of the International Top. Meeting on Remote Systems and Robotics in Hostile Environments*, 630-637, Pasco, Washington (1987).
2. G. Streiff, et al., "Association of remote dexterity and remote lifting for maintenance in fuel reprocessing industry," *Proc. of the International Top. Meeting on Remote Systems and Robotics in Hostile Environments*, 197-203, Gatlinburg, Tennessee (1984).
3. N. Kircanski and A. Goldenberg, "An experimental study of nonlinear stiffness, hysteresis, and friction effects in robot joints with harmonic drives and torque sensors," *Int. Journal of Robotics Research*, 16, 2, 214-239 (1997).
4. J. J. Fisher, et al., "Development of telerobotic system for handling of contaminated process equipment," *Proc. of the International Top. Meeting on Remote Systems and Robotics in Hostile Environments*, 78-85, Pasco, Washington (1987).
5. S. H. Ahn, J. S. Yoon and S. J. Lee, "A force reflecting control scheme for telemanipulators with high reduction ratio joint," *Robotica*, 20, 1, 69-79 (2002).
6. M. V. Kothare, P. J. Campo, M. Morari and C. N. Nett, "A unified framework for the study of anti-windup designs," *Automatica*, 30, 12,

11869-1883 (1994).

7. M. Uebel, M. Ali and I. Minis, "The effect of bandwidth on telerobot system performance," *IEEE Trans. on Systems, Man and Cybernetics*, 24, 2, 342-348 (1994).
8. M. W. Spong and M. Vidyasagar, Robot dynamics and control, John Wiley & Sons, Inc. (1989).
9. P. McKerrow, Introduction to robotics, Addison-Wesley, (1986).